ICSV13 - Vienna
The Thirteenth International Congress on Sound and Vibration
Vienna, Austria, July 2-6, 2006

A PHYSICAL INTERPRETATION OF FREQUENCY DEPENDENT BOUNDARY CONDITIONS IN A DIGITAL WAVEGUIDE MESH

José Escolano* and Finn Jacobsen

Acoustic Technology, Oersted·DTU
Technical University of Denmark, Building 352, Oersteds Plads,
DK-2800 Kgs. Lyngby, Denmark
fja@oersted.dtu.dk

Abstract

Digital Waveguide Mesh (DWM) is a popular method for time domain modelling of sound fields. DWM consists of a recursive digital filter structure where a D'Alembert solution of the wave equation is propagated. One of the attractive characteristics of this method is related to the simplicity of incorporating frequency dependent boundary conditions. Assuming that the reflecting surfaces are linear and time-invariant, their impedances (and thus, their reflection factors) can be simulated by means of digital filtering. So far such digital filters have been designed to provide reflection factors corresponding to the impedance of the boundaries for normal sound incidence. However, the resulting model of the boundary does not agree with the behaviour of a locally reacting surface, and this can give rise to contradictions in the physical interpretation of the reflected sound field. This paper analyses the behaviour of frequency dependent boundary conditions in DWN in order to obtain a physical interpretation of the simulated impedance surfaces. The interpretation is validated by several examples.

INTRODUCTION

Many problems in room acoustics can be solved by means of numerical time-domain methods. Such methods provide fast and accurate solutions and their importance has grown with the power of computers.

Among the different methods for acoustic simulations, the Digital Waveguide Mesh (DWM) [1] should be mentioned because it offers some advantages compared with other time-domain methods. These advantages are related with the capacity of applying digital signal processing theory directly to the method. This makes it possible to take account of, e. i., air absorption and frequency dependent boundary conditions.

The ability of modelling frequency dependent reflections can be a key point for choosing this method instead of others. With DWM one can model the reflections using digital filters [2] that represent frequency dependent reflection factors. However, the resulting boundary filters and thus reflection factors are not dependent on the angle of incidence in the same way as the corresponding locally reacting surfaces [3]. This paper analyses how well the DWM model agrees with the locally reacting impedance model. The model analysed in this paper is a 2D model; a 3D model follows the same analysis.

DIGITAL WAVEGUIDE MESH

Theory

The theory of DWM is based on decomposing the solution to the wave equation into travelling (or diverging and converging) waves, as in the D'Alembert solution. In an ideal lossless medium, the wave equation can be implemented by means of pure delays, and the total sound field is obtained by adding travelling wave components. In the simple 1D case, the D'Alembert solution is written as

$$\psi(x,t) = \psi^{-}(x-ct) + \psi^{+}(x+ct). \tag{1}$$

This case can be seen as a decomposition of a direct wave, ψ^{+}, and a reflected wave, ψ^{-}, in a medium with the speed of sound c. Each travelling wave can be simulated by a shift register using pure or fractional delays. In this way, the digital waveguide model is obtained by sampling both space and time. Spatial sampling points are known as *scattering junctions*.

In the multidimensional case each scattering junction, situated at position $\mathbf{s}$, is linked by means of bi-directional unit-delays to N neighbouring scattering junctions defined with index κ where $\kappa = 1, \ldots, N$.

In Fig. 1(a) a scheme of the DWM method is presented. The pressure $p(\mathbf{s}, n)$ is situated at the centre of the figure, and it is surrounded by N neighbouring scattering junctions that are represented by $p(\mathbf{s}_\kappa, n)$ ($\kappa = 1, \ldots, N$). The particle velocity $u(\mathbf{s}, n)$ follows the same notation and the scheme is equivalent. Figure 1(b) represents a DWM based on digital signal processing theory, where scattering junctions are joined using digital delays.

Let the signal $p_\kappa^{+}(\mathbf{s}, n)$ be an incoming signal from the neighbouring junction and $p_\kappa^{-}(\mathbf{s}, n)$ represent an outgoing component. Note that delay lines $p_\kappa^{+}(\mathbf{s}, n)$ and $p_\kappa^{-}(\mathbf{s}, n)$ join $p(\mathbf{s}, n)$ and $p(\mathbf{s}_\kappa, n)$ (see Fig. 1(a)). As the delay elements are bi-directional, the pressure is defined as

$$p_\kappa(\mathbf{s}, n) = p_\kappa^{+}(\mathbf{s}, n) + p_\kappa^{-}(\mathbf{s}, n). \tag{2}$$

In a lossless scattering, the Kirchhoff laws must hold,

1. The sum of incoming particle velocities is equal to the sum of outgoing particle velocities at each junction

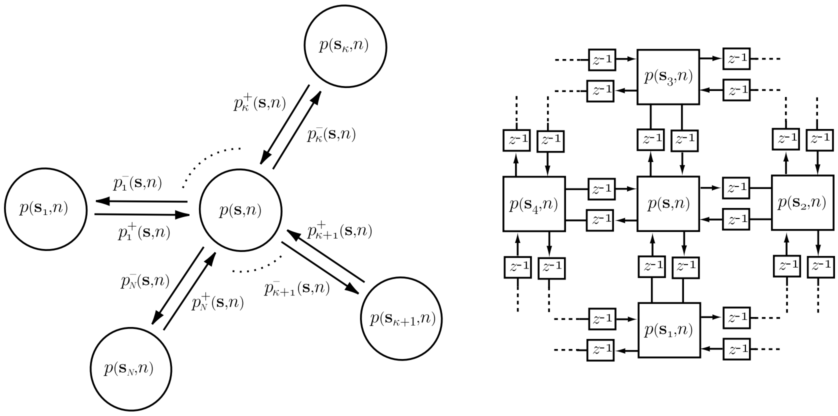

Figure 1: a) Scattering junctions scheme in a Digital Waveguide Mesh. b) Implementation of a DWM with digital signal processing theory

2. The pressures in all crossing waveguides are equal at the junction

According to these rules and assuming an homogeneous medium with a characteristic impedance of $Z_\kappa(\mathbf{s}) = \rho c$, $\forall\kappa$) the sound pressure at a scattering junction is obtained as

$$p(\mathbf{s}, n) = \frac{2}{N} \sum_{\kappa=1}^{N} p^+_\kappa(\mathbf{s}, n). \tag{3}$$

¿From the second Kirchhoff law the reflected component can be obtained as

$$p^-_\kappa(\mathbf{s}, n) = p(\mathbf{s}, n) - p^+_\kappa(\mathbf{s}, n). \tag{4}$$

In the next time step, the outgoing components are incoming in the opposite direction. This can be expressed as

$$p^+_\kappa(\mathbf{s}_\kappa, n+1) = p^-_\kappa(\mathbf{s}, n), \tag{5}$$

where $p^+_\kappa(\mathbf{s}_\kappa, n)$ represents the incoming delay line with respect to the scattering junction $p(\mathbf{s}_\kappa, n)$ that links with $p(\mathbf{s}, n)$.

For the 2D case and for cartesian coordinates, the number of bi-directional delay lines is 4, whereas in 3D simulations it is 6. More complex and efficient structures can also be implemented [4].

It should be mentioned that the spatial $(\Delta x, \Delta y)$ and temporal sampling (Δt) cannot be left to chance; a relation between them must exist. In the DWM case, it follows the same relation as with the finite difference time domain method [5]. This stability condition is known as the Courant condition and it is defined as

$$c\Delta t \leq \frac{1}{\sqrt{\left(\frac{1}{\Delta x}\right)^2 + \left(\frac{1}{\Delta y}\right)^2}}. \tag{6}$$

Frequency Dependent Boundary Conditions in a Digital Waveguide Mesh

One of the advantages of the DWM is the ease with which frequency dependent boundary conditions can be included in the simulation. This is done by connecting a boundary filter in each node representing the reflecting coefficient. This makes it possible to have different impedance conditions at each point of the boundaries. Figure 2 represents a scheme of the interaction of 2D DWM with the boundary filters.

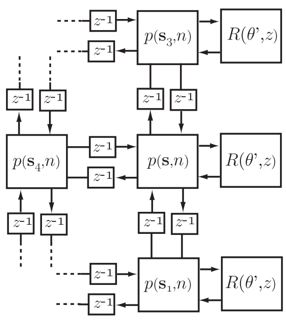

Figure 2: Interaction between DWM and boundary filters

However, a locally reacting surface with a specific impedance of $Z(\omega)$ has a plane wave reflecting factor that depends on the angle of incidence,

$$R(\theta', \omega) = \frac{Z(\omega)\cos\theta' - \rho c}{Z(\omega)\cos\theta' + \rho c}. \tag{7}$$

Since the angle of incidence θ' is generally unknown normal incidence is usually assumed [2]. In other words, with a given analytical impedance model (or with an impedance determined experimentally), the reflecting factor filter is obtained by assuming that θ' is zero.

ANALYSIS OF BOUNDARY CONDITIONS IN DWM

In order to analyse the behaviour of the impedance model in DWN, an impedance boundary is considered at $x = 0$. The other boundaries are assumed to be non-reflecting. Consider a discrete broadband plane wave $p_i(\mathbf{s}, n)$, with particle velocity $u_{x_i}(\mathbf{s}, n) = p_i(\mathbf{s}, n)\cos(\theta)/(\rho c)$.

If the reflecting factor of the model is defined as $\hat{r}(\theta, n)$ in the time domain, the reflected pressure is a time convolution, $p_r(\mathbf{s}, n) = p_i(\mathbf{s}, n) * \hat{r}(\theta, n)$. Information about the reflecting factor of the particle velocity is not directly available, but some of the results of the Finite Difference method [5] can be useful in this analysis.

A finite difference formulation of the Euler equation of motion is

$$u_x(i,j,n) = u_x(i,j,n-1) + \frac{1}{\rho}\frac{\Delta t}{\Delta x}(p(i+1,j,n) - p(i,j,n)) \tag{8}$$

Centred at $x = 0$ and decomposing $p(0,j,n)$ into reflected and reflected components, Eq. (8) becomes

$$u_x(0,j,n) = u_x(0,j,n-1) + \frac{1}{\rho}\frac{\Delta t}{\Delta x}(p(1,j,n) - p_i(0,j,n) * (\delta(n) + \hat{r}(\theta,n))). \tag{9}$$

This expression can easily be separated into direct and reflected parts (in the absence of reflection, only the incident part exists). In this case, it is the reflected part that is interesting,

$$u_{x_r}(0,j,n) = -\frac{1}{\rho}\frac{\Delta t}{\Delta x}(p_i(0,j,n) * \hat{r}(\theta,n)). \tag{10}$$

The fraction $\Delta t/\Delta x$ can provide some information if certain algebraic modifications are carried out. Assuming equality in the Courant formula (Eq. (6)), the fraction $\Delta t/\Delta x$ is

$$\frac{\Delta t}{\Delta x} = \frac{\frac{1}{\Delta x}}{c\sqrt{\left(\frac{1}{\Delta x}\right)^2 + \left(\frac{1}{\Delta y}\right)^2}} = \frac{\Delta y}{c\sqrt{\Delta x^2 + \Delta y^2}}. \tag{11}$$

The fraction $\Delta y/\sqrt{\Delta x^2 + \Delta y^2}$ can be seen to be identical with the cosine of the angle α that forms the diagonal direction with respect to the mesh coordinate system. Finally, the total particle velocity component (incident plus reflected) in x-direction at $x = 0$ becomes

$$u_x(0,j,n) = \frac{p_i(0,j,n)}{\rho c}\cos\theta - \frac{p_i(0,j,n) * \hat{r}(\theta,n)}{\rho c}\cos\alpha. \tag{12}$$

In order to calculate the reflecting factor it is necessary to obtain the impedance at $x = 0$ (the ratio of the pressure to the particle velocity) in the Z-transformed domain. Finally, the reflecting factor for the DWM becomes $\hat{R}(\theta,z) = \mathcal{Z}\{\hat{r}(\theta,n)\}$ which equals

$$\hat{R}(\theta,z) = \frac{Z(z)\cos\theta - \rho c}{Z(z)\cos\alpha + \rho c}, \tag{13}$$

However, the impedance $Z(z)$ related with the reflecting factor filter is forced as a boundary condition. Substituting Eq. (7) into Eq. (13) gives a relation between the expected reflecting factor and the one that is obtained,

$$\hat{R}(\theta,z) = \frac{R(\theta',z)(\frac{\cos\theta}{\cos\theta'} + 1) + (\frac{\cos\theta}{\cos\theta'} - 1)}{R(\theta',z)(\frac{\cos\alpha}{\cos\theta'} - 1) + (\frac{\cos\alpha}{\cos\theta'} + 1)} \tag{14}$$

Equation (14) shows that the best agreement is obtained when the angle of incidence (θ), the angle selected in the filter design (θ'), and the diagonal angle in the mesh (α) are the same. Note that α is determined by the mesh; however, at least the impedance model can be improved at some angles by forcing $\theta' = \alpha$. To summarise, according to the WDM impedance model (Eq. (13)) the reflecting factor is dependent on the angle of sound incidence, but not in the same manner as a real locally reacting impedance surface is.

RESULTS

To examine the behaviour of the DWM approximation to a locally reacting impedance, some DWM implementations have been carried out. A 2D rectangular mesh with 200×200 ($\Delta x = \Delta y$) cells is designed with a boundary filter at $x = 0$, and the other boundaries are absorbing boundary conditions [6]. The sampling frequency is 40 KHz and the excitation is a Gaussian pulse with a bandwidth of 5 kHz. The impedance is modelled as a hard-backed layer of porous material, described by the Delany and Bazley expressions [7]. In the following simulations a 0.1 m layer of porous material with a flow resistivity of 1000 kg/m^3/s. The coefficients of the digital filter are defined according to Prony's algorithm with an IIR digital filter of 40th order using the analytical response of the impedance model. Figure 3 shows the reflecting factor of a locally reacting impedance surface at different angles of incidence, calculated from Eq. (7) and the impedance described above.

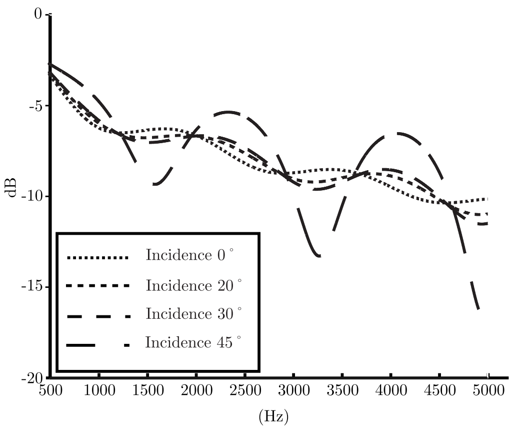

Figure 3: Reflecting factor of a locally reacting impedance at different angles of plane wave incidence.

As mentioned in the foregoing, the boundary filter can be designed with a degree a freedom, the parameter θ'. In the literature this parameter has invariably been selected as 0; in other words, the reflection factor that occurs for normal incidence has been used. However, as shown above, a better approximation to a locally reacting surface is obtained by choosing $\theta' = \alpha$, which in this case means $\alpha = \pi/4$. Both designs are presented in Fig. 4.

Figure 4(a) shows different reflection factors obtained in a DWM when θ'=0. The figure demonstrates that the resulting reflection factors disagree with the designed filter. The largest differences occur when the sound incidence is in the normal direction. For other angles of incidence a behaviour similar to that of the filter can be observed. In addition to these

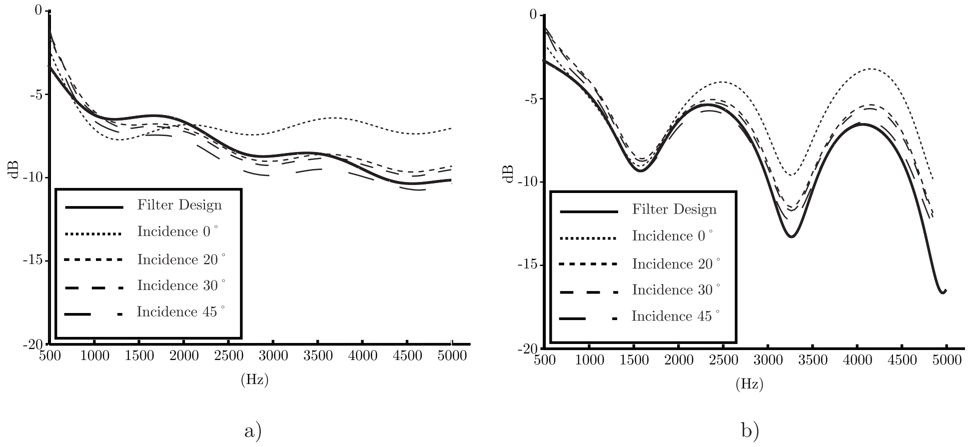

Figure 4: (a) Reflection factor with θ'=0; (b) reflection factor with $\theta' = \pi/4$.

differences some frequency shifts can be seen. These frequency shifts are due to the inherent (artificial) dispersion of the DWM algorithm. The strongest dispersion occurs for normal incidence.

Figure 4(b) represents the case where $\theta' = \pi/4$. It can be seen that the differences between the results and the design for most angles of incidence are moderate, and it is also apparent that the frequency dispersion is reduced compared with the case where $\theta' = 0$. It is well known that the dispersion of the DWM method is minimised for the incidence angle α.

Both figures demonstrate that the general model for boundary conditions in the DWM method do not correspond to a locally reacting surface, although there is a dependence of the angle of incidence. The deviations from the behaviour of a locally reacting impedance surface can be predicted from Eq. (14).

CONCLUSIONS

The behaviour of the boundary filter in the Digital Waveguide Mesh method has been analysed. In DWM the boundary conditions are implemented with digital filters with transfer functions corresponding to the desired reflecting factors. A locally reacting impedance surface was assumed. However, contradictions appear when the boundary conditions are designed by forcing the reflecting factor to some assumed angle of incidence.

The results show that although the DWM method gives an angle-dependent reflection factor, the model does not correspond to a locally reacting surface in general. It is only in specific cases that the results will agree with this model. Furthermore, it is necessary to include one degree of freedom in the design of the boundary filter. This parameter can be used to align the dependence of the angle of incidence to a specific angle. Some examples have been presented that demonstrate not only the disagreement with the locally reacting model, but also how the parameter θ can influence in the behaviour of the boundary conditions.

ACKNOWLEDGMENTS

The first author's stay at DTU has been made possible by a European Doctorate in Sound and Vibration Studies (EDSVS) Marie Curie scholarship from the EC.

REFERENCES

References

[1] J.O. Smith III, "Physical modelling using digital waveguides," *Computational Music J.*, **16**(4), 74–91 (1992).

[2] J. Huopaniemi et al., "Modelling of reflections and air absorption in acoustical spaces – a digital filter design approach", *IEEE Workshop on Applications of Signal Proccesing to Audio and Acoustics (WASPAA'97)*, New York, USA (1997).

[3] H. Kuttruff, *Room Acoustics* 4th ed. (Spon Press, New York, 2000).

[4] D.T. Murphy and D.M. Howard, "Digital waveguide modelling of room acoustics: Comparing mesh topologies," in *Proc. of 25th Euromicro Conference (Euromicro'99)*, **02**(2), preprint 2082 (1999).

[5] D. Botteldooren, "Finite-difference time-domain simulation of low-frequency room acoustic problems," *J. Acoust. Soc. Am.* **98**, 3302–3308 (1995).

[6] D.T. Murphy and J. Mullen, "Digital waveguide mesh modelling of room acoustics: Improved anechoic boundaries", *6th Conference in Digital Audio Effects (DAFX-02)*, pp. 163-168, Hamburg, Germany, Sep. 2002.

[7] M.E. Delany and E.N. Bazley, "Acoustical properties of fibrous absorbent materials", *Applied Acoustics* **3**, 105–116 (1970).